

1    **Title:**

2    MetaDome: Pathogenicity analysis of genetic variants through aggregation of homologous  
3    human protein domains

4

5    **Authors and affiliations:**

6    Laurens Wiel<sup>1,2</sup>, Coos Baakman<sup>2</sup>, Daan Gilissen<sup>1,3</sup>, Joris A. Veltman<sup>4,5</sup>, Gerrit Vriend<sup>2</sup> and  
7    Christian Gilissen<sup>4</sup>

8

9    1. Department of Human Genetics, Radboud Institute for Molecular Life Sciences, Radboud  
10   University Medical Center, Nijmegen, 6525 GA, the Netherlands

11   2. Centre for Molecular and Biomolecular Informatics, Radboud Institute for Molecular Life  
12   Sciences, Radboud University Medical Center, Nijmegen, 6525 GA, the Netherlands

13   3. Bio-informatica, HAN University of Applied Sciences, Nijmegen, 6525 EN, the Netherlands

14   4. Department of Human Genetics, Donders Institute for Brain, Cognition and Behaviour,  
15   Radboud University Medical Center, Nijmegen, 6525 GA, the Netherlands

16   5. Institute of Genetic Medicine, International Centre for Life, Newcastle University, Newcastle  
17   upon Tyne, NE1 3BZ, United Kingdom

18

19   Corresponding author: Christian Gilissen

20 **Abstract (199/200)**

21 The growing availability of human genetic variation has given rise to novel methods of  
22 measuring genetic tolerance that better interpret variants of unknown significance. We recently  
23 developed a novel concept based on protein domain homology in the human genome to improve  
24 variant interpretation. For this purpose we mapped population variation from the Exome  
25 Aggregation Consortium (ExAC) and pathogenic mutations from the Human Gene Mutation  
26 Database (HGMD) onto Pfam protein domains. The aggregation of these variation data across  
27 homologous domains into meta-domains allowed us to generate base-pair resolution of genetic  
28 intolerance profiles for human protein domains.

29 Here we developed MetaDome, a fast and easy-to-use web service that visualizes meta-domain  
30 information and gene-wide profiles of genetic tolerance. We updated the underlying data of  
31 MetaDome to contain information from 56,319 human transcripts, 71,419 protein domains,  
32 12,164,292 genetic variants from gnomAD, and 34,076 pathogenic mutations from ClinVar.  
33 MetaDome allows researchers to easily investigate their variants of interest for the presence or  
34 absence of variation at corresponding positions within homologous domains. We illustrate the  
35 added value of MetaDome by an example that highlights how it may help in the interpretation of  
36 variants of unknown significance. The MetaDome web server is freely accessible at  
37 <https://stuart.radboudumc.nl/metadome>.

38 **Key Words**

39 Genetic variation; pathogenicity; web server; protein domain homology; genetic tolerance; meta-  
40 domains; gnomAD; ClinVar; Pfam

## 41      **Introduction**

42      The continuous accumulation of human genomic data has spurred the development of new  
43      methods to interpret genetic variants. There are many freely available web servers and services  
44      that facilitate the use of these data by non-bioinformaticians. For example, the ESP Exome  
45      Variant Server (Fu et al., 2012; NHLBI GO Exome Sequencing Project (ESP), 2011) and the  
46      Genome Aggregation Database (gnomAD) browser (Karczewski et al., 2017; Lek et al., 2016)  
47      help locate variants that occur frequently in the general population. These services are used for  
48      the interpretation of unknown variants based on the assumption that variants occurring frequently  
49      in the general population are unlikely to be relevant for patients with Mendelian disorders (Amr  
50      et al., 2016). There are also methods that derive information from these large human genetic  
51      databases. For example genetic intolerance, which is commonly used to interpret variants of  
52      unknown significance by assessing whether variants stand out because they occur in regions that  
53      are genetically invariable in the general population (Ge et al., 2016; Gussow et al., 2016).  
54      Examples of such methods are RVIS (Petrovski, Wang, Heinzen, Allen, & Goldstein, 2013) and  
55      subRVIS (Gussow, Petrovski, Wang, Allen, & Goldstein, 2016). The strongest evidence for the  
56      pathogenicity of a genomic variant comes from the presence of that variant in any of the  
57      clinically relevant genetic variant databases such as the Human Gene Mutation Database  
58      (HGMD) (Stenson et al., 2017) or the public archive of clinically relevant variants (ClinVar)  
59      (Landrum et al., 2016). These databases are gradually growing in the amount of validated  
60      pathogenic information.

61      Another way to provide evidence for the pathogenicity of a genomic variant is to observe the  
62      effect of that variant in homologous proteins across different species. Mutations at corresponding  
63      locations in homologous proteins are found to result in similar effects on protein stability

64 (Ashenberg, Gong, & Bloom, 2013). Finding homologous proteins is one the key applications of  
65 BLAST (Altschul, Gish, Miller, Myers, & Lipman, 1990). Transferring information between  
66 homologous proteins is one of the oldest concepts in bioinformatics, and can be achieved by  
67 performing a multiple sequence alignment (MSA) and locating equivalent positions between the  
68 protein sequences. We have previously used this concept and showed that it also holds for  
69 homologous Pfam protein domain relationships within the human genome. We found that ~71-  
70 72% of all disease-causing missense variants from HGMD and ClinVar occur in regions  
71 translating to a Pfam protein domain and observed that pathogenic missense variants at  
72 equivalent domain positions are often paired with the absence of population-based variation and  
73 *vice versa* (Wiel, Venselaar, Veltman, Vriend, & Gilissen, 2017). By aggregating variant  
74 information over homologous protein domains, the resolution of genetic tolerance per position is  
75 increased to the number of aligned positions. Similarly, the annotation of pathogenic variants  
76 found at equivalent domain positions also assists the interpretation of variants of unknown  
77 significance. We realized that this type of information could be of great benefit to the genetics  
78 community and therefore developed MetaDome.

79 MetaDome is a freely available web server that uses our concept of 'meta-domains' (i.e.  
80 aggregated homologous domains) to optimally use the information from population-based and  
81 pathogenic variation datasets without the need of a bioinformatics intermediate. MetaDome is  
82 easy to use and utilizes the latest population datasets by incorporating the gnomAD and ClinVar  
83 datasets.

84 **Results**

85 **Accessibility**

86 The MetaDome web server is freely accessible at <https://stuart.radboudumc.nl/metadome>.

87 MetaDome features a user-friendly web interface and features a fully interactive tour to get  
88 familiar with all parts of the analysis and visualizations.

89 All source code and detailed configuration instructions are available in our GitHub repository:

90 <https://github.com/cmbi/metadome>.

91 **The underlying database: a mapping between genes and proteins**

92 The MetaDome web server queries genomic datasets in order to annotate positions in a protein or  
93 a protein domain. Therefore, the server needs access to genomic positional information as well as  
94 protein sequence and protein domain information. The database maps GENCODE gene  
95 translations to entries in the UniProtKB/Swiss-Prot databank in a per-position manner and  
96 corresponding protein domains or genomic variation. With respect to our criteria to map gene  
97 translations to proteins (**Methods; creating the mapping database**), 42,116 of the 56,319 full-  
98 length protein-coding GENCODE Basic transcripts for 19,728 human genes are linked to 33,492  
99 of the 42,130 Swiss-Prot human canonical or isoform sequences. Of the total 591,556 canonical  
100 and isoform sequences present in Swiss-Prot, 42,130 result from the Human species. The  
101 resulting mappings contain 32,595,355 unique genomic positions that are linked to 19,226,961  
102 residues in Swiss-Prot protein sequences.

103 71,419 Pfam domains are linked to 30,406 of the Swiss-Prot sequences in our database. Of these  
104 Pfam domain instances, 5,948 are from a unique Pfam domain family and 3,334 of these families  
105 have two or more homologues and are therefore suitable for meta-domain construction. Thus, by

106 incorporating every protein-coding transcript, instead of only the longest ones, we increase the  
107 previously 2,750 (Wiel et al., 2017) meta-domains to 3,334. These meta-domains, on average,  
108 consist of 16 human protein domain homologues with a protein sequence length of 158 residues.  
109 **Table 1** summarizes the counting statistics for sequences, domains, etc.

110 **Table 1.** Statistics on the number of entries present in GENCODE, Swiss-Prot, and our mapping  
111 database.

Database	What	# of entries
GENCODE	Protein-coding genes	20,345
MetaDome	Protein-coding genes	19,728
GENCODE	Protein-coding transcripts	57,005
MetaDome	Protein-coding transcripts	56,319
Swiss-Prot	Canonical and isoform protein sequences	591,556
Swiss-Prot	Human canonical and isoform protein sequences	42,130
MetaDome	Gene translations identically mapped to a canonical or isoform protein sequence	42,116
MetaDome	Canonical and isoform protein sequences	33,492
MetaDome	Pfam protein domain regions	71,419
MetaDome	Unique Pfam protein domain families	5,948
MetaDome	Unique Pfam protein domain families with two or more within-human occurrences	3,334
MetaDome	Chromosome to protein position mappings	70,261,143
MetaDome	Unique chromosome positions	32,595,355

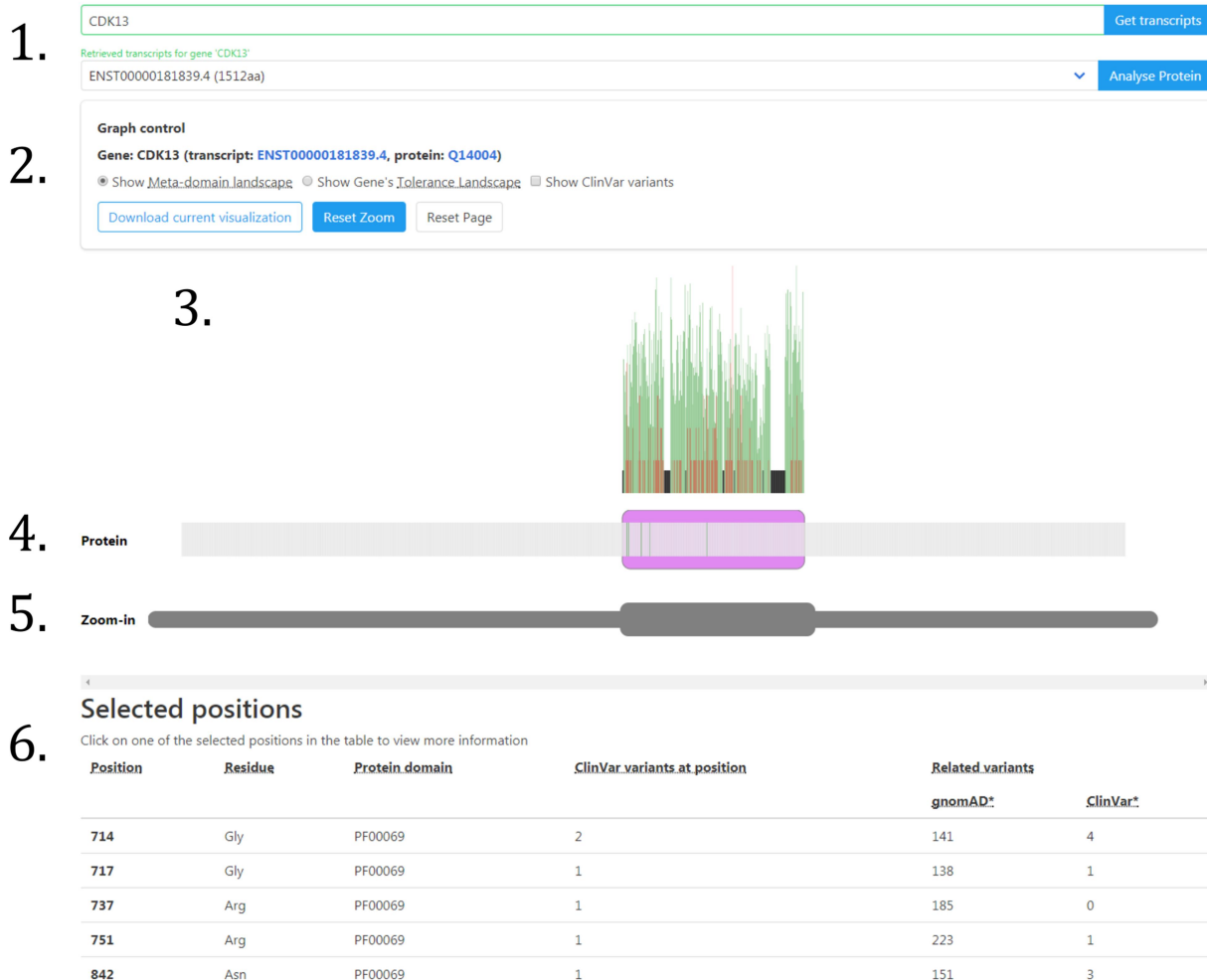
MetaDome	Unique residues (as part of a protein)	19,226,961
MetaDome	Unique protein sequences with at least one Pfam domain annotated	30,406

112 **How to use the MetaDome web server**

113 At the welcome page users are offered the option to start an interactive tour or start with the  
114 analysis. The navigation bar at the top is available throughout all web pages in MetaDome and  
115 allow for further navigation to the ‘About’, ‘Method’, ‘Contact’ page (**Supp. Figure S1**). The  
116 user can fill in a gene symbol in the ‘gene of interest’ field and is aided by an auto-completion to  
117 help you find your gene of interest more easily (**Supp. Figure S2**). Clicking the ‘Get transcripts’  
118 fills all GENCODE transcripts for that gene in the dropdown box. Only the transcripts that are  
119 mapped to a Swiss-Prot protein can be used in the analysis, the others are displayed in grey  
120 (**Supp. Figure S3**).

121 Clicking the ‘Start Analysis’ button starts an extensive query to the back-end of the web server  
122 for the selected transcript. Firstly, all the mappings are retrieved for the transcript of interest.  
123 Secondly, the entire transcript is annotated with ClinVar and gnomAD single nucleotide variants  
124 (SNVs) and Pfam domains. Thirdly, if there are any Pfam domains suitable for meta-domain  
125 relations then all mappings for those regions are gathered and annotated with ClinVar and  
126 gnomAD variation (**methods; Composing a meta-domain**).

127



128

129 **Figure 1.** MetaDome web server result for the gene *CDK13*

130 The result provided by the MetaDome web server for the analysis of gene *CDK13* with transcript  
131 ENST00000181839.4, as provided in 1.). In 2.), there is additional information that the  
132 translation of this transcript corresponds to Swiss-Prot protein Q14004. Here also various  
133 alternative visualizations can be selected. The visualization starts by default in the ‘meta-domain  
134 landscape’, a mode selectable in the graph control in 2.). The landscapes are visualized in 3.),  
135 and in the meta-domain landscape the domain regions are annotated with missense variation

136 counts found in homologous domains as bar plots. The schematic protein representation, located  
137 at 4.), is per-position selectable, and the domains are presented as purple blocks. Selected  
138 positions are highlighted in green. The ‘Zoom-in’ section at 5.) features a selectable greyed-out  
139 copy of schematic protein representation that can zoom-in on any part of the protein. Any  
140 selected positions are in the list of selected positions in 6.). Here more information can be  
141 obtained by clicking on one of these positions. A detailed description of the functionality of each  
142 component is described in **Table 2**.

---

143

144 The web-page provided to the user as a result of the ‘Analyse Protein’ can best be explained  
145 using an example. Therefore, we have generated this result for gene *CDK13* for transcript  
146 ‘ENST00000181839.4‘ (**Figure 1**). The result page features four main components that we will  
147 describe from top to bottom. Located at the top is the graph control field. Directly below the  
148 graph control is the landscape view of the protein. Below the landscape view, a schematic and  
149 interactive representation of the protein and an additional representation of the protein which  
150 controls the zooming option. Lastly, at the bottom of the page there is the list of selected  
151 positions. All of these components are interactive and the various functionalities are described in  
152 **Table 2**.

153 Another way to use population-based variation in the context of the entire protein is via the  
154 tolerance landscape representation in MetaDome that can be selected in the graph control  
155 component (**Figure 1.2**). The tolerance landscape depicts a missense over synonymous ratio  
156 (also known as  $K_a/K_s$  or  $d_N/d_S$ ) over a sliding window of 21 residues over the entirety of the  
157 protein of interest (e.g. calculated for ten residues left and right of each residue) based on the

158 gnomAD dataset (**methods**; **Computing genetic tolerance and generating a tolerance**  
159 **landscape; Figure 2A**). Previously, the  $d_N/d_S$  metric has been used by others and us to measure  
160 genetic tolerance and predict disease genes (Ge, Kwok, & Shieh, 2015; Gilissen et al., 2014;  
161 Lelieveld et al., 2017), and it is suitable for measuring tolerance in regions within genes (Ge et  
162 al., 2016).

163

164 **Table 2.** Descriptions of the various functionalities on the MetaDome result page.

Component	Functionality
Gene and transcript input field (Figure 1.1)	<ul style="list-style-type: none"><li>• Input of gene of interest</li><li>• Retrieving transcripts for gene of interest</li><li>• Selecting a transcript</li><li>• Starting the analysis for selected transcript</li></ul>
Graph control field (Figure 1.2)	<ul style="list-style-type: none"><li>• Toggling between different landscape representations</li><li>• Reset the zoom on the landscape</li><li>• Reset the web page</li><li>• Toggle ClinVar variants to be displayed in the schematic protein</li><li>• Download the visual representation</li></ul>
Landscape view (Figure 1.3)	<ul style="list-style-type: none"><li>• Displays the meta-domain landscape</li><li>• Displays the tolerance landscape</li></ul>
Schematic protein	<ul style="list-style-type: none"><li>• Displays a schematic representation of the gene's protein</li></ul>

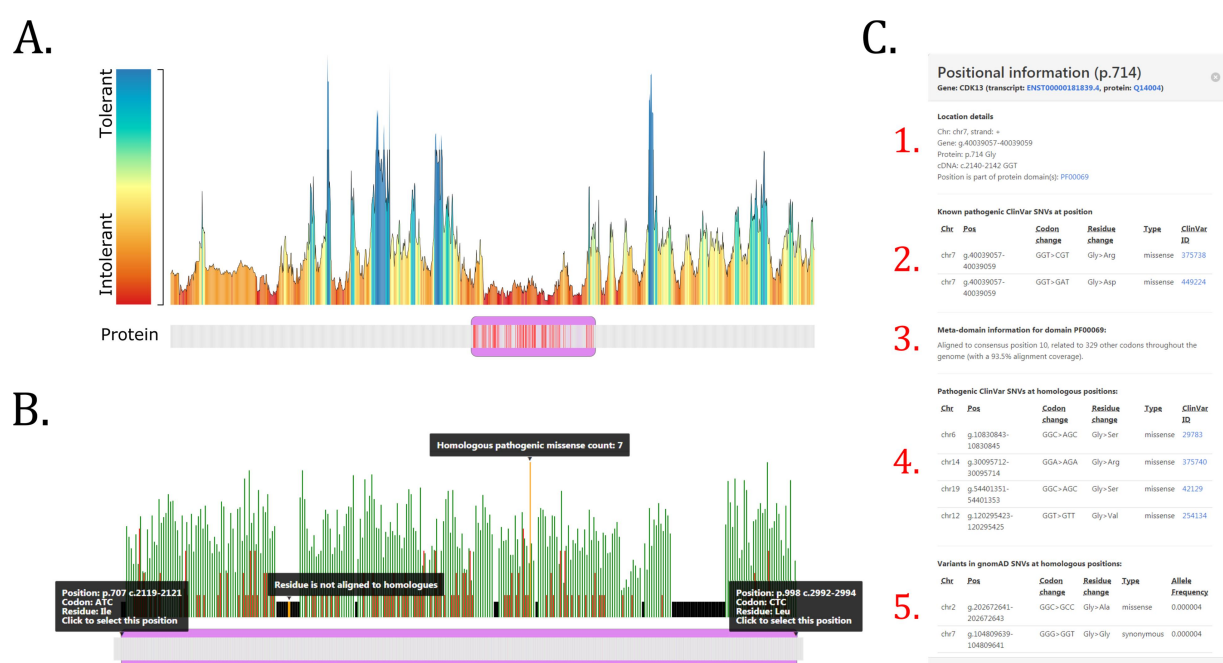
(Figure 1.4)	<p>with Pfam protein domains annotated</p> <ul style="list-style-type: none"><li>• Hovering over a position displays positional information</li><li>• Clicking on a position highlights the position and adds the position to the list of ‘Selected Positions’</li><li>• Controls the zooming of particular parts of the protein (Figure 1.5)</li></ul>
Selected Positions (Figure 1.6)	<ul style="list-style-type: none"><li>• Displays any positions selected in the schematic protein</li><li>• Displays per selected position: if that position is part of a Pfam protein domain, any known gnomAD or ClinVar variants present at this position, and any variants that are homologously related to this position</li><li>• Provides more detailed information as a pop-up when clicking on one of the positions in this list.</li></ul>

165

166 **An example of using the MetaDome web server for variant interpretation**

167 The MetaDome analysis result for *CDK13* (Figure 1) is the longest protein coding transcript for  
168 *CDK13* with a protein sequence length of 1,512 amino acids. In the resulting schematic protein  
169 representation we can observe the Pkinase Pfam protein domain (PF00069) between positions  
170 707 and 998 as the only protein domain in this gene (Figure 2B). The Pkinase domain is highly  
171 prevalent throughout the human genome with as many as 779 homologous occurrences in human  
172 proteins, of which 353 are unique genomic regions. It is the 8th most occurring domain in our  
173 mapping database. The meta-domain landscape is the default view mode and shows any  
174 missense variation found in homologous domain occurrences throughout the human genome.

175 Population-based (gnomAD) missense variation is displayed in green and pathogenic (ClinVar)  
176 missense variation is annotated in red bars, with the height of the bars depicting the number of  
177 variants found at each position (**Figure 2B**).



178

179 **Figure 2.** Examples of a MetaDome analysis for the gene *CDK13*

180 **A.)** The tolerance landscape depicts a missense over synonymous ratio calculated as a sliding  
181 window over the entirety of the protein (**methods; Computing genetic tolerance and**  
182 **generating a tolerance landscape**). The missense and synonymous variation are annotated from  
183 the gnomAD dataset and the landscape provides some indication of regions that are intolerant to  
184 missense variation. In this *CDK13* tolerance landscape the Pkinase Pfam protein domain  
185 (PF00069) in purple can be clearly seen as intolerant if compared to other parts in this protein.  
186 The red bars in the schematic protein representation correspond to pathogenic ClinVar variants  
187 found in this gene and in homologous protein domains. All of these variants are contained in the  
188 intolerant region of the landscape.

189 **B.)** A zoom-in on the meta-domain landscape for *CDK13*. The Pkinase Pfam protein domain  
190 (PF00069) is located between protein positions 707 and 998 and annotated as a purple box in the  
191 schematic protein representation. The meta-domain landscape displays a deep annotation of the  
192 protein domain: the green (gnomAD) and red (ClinVar) bars correspond to the amount of  
193 missense variants found at aligned homologous positions. Unaligned positions are annotated as  
194 black bars. All of this information is displayed upon hovering over these various elements.

195 **C.)** The positional information provides a detailed overview of a position from the ‘Selected  
196 Positions’ list, especially if that position is aligned to domain homologues. Here, for position  
197 p.Gly714 we can observe in 1.) the positional details for this specific protein position. In 2.) is  
198 any known pathogenic information for this position. We can observe here that for this position  
199 there are two known pathogenic missense variants. In 3.) meta-domain information is displayed  
200 and we can observe that p.Gly714 is aligned to consensus position 10 in the Pkinase Pfam  
201 protein domain and related to 329 other codons. This consensus position has an alignment  
202 coverage of 93.5% for the meta-domain MSA. There are also four pathogenic variants found in  
203 ClinVar on corresponding homologous positions as can be seen in 4.) and in 5.) there is an  
204 overview of all corresponding variants found in gnomAD.

---

205

206 If the ‘Show ClinVar variants’ is toggled in the graph control field, we may observe that all  
207 known pathogenic information is highlight positions in the schematic protein in a red colour and  
208 for this example is located in the protein domain (**Figure 2A**). All ClinVar variants annotated to  
209 the gene are displayed this way in red. Additionally, any ClinVar variants that are present at  
210 homologous positions are also displayed in red. In total six known disease causing SNVs are

211 present in the *CDK13* gene itself according to ClinVar, and these all fall within the Pkinase  
212 protein domain. All of these are missense variants. If we add variants found in homologous  
213 domains there are 64 positions with one or more reported pathogenic variants (**Supp Data S1**).  
214 Four of these positions overlap with the positions on which ClinVar variants were found in the  
215 gene itself and on position p.883 (**Supp. Figure S4**) we can observe a peak of eight missense  
216 variants annotated from other protein domains.

217 MetaDome helps to look in more detail to a position of interest. If we do this for protein position  
218 714 (**Figure 2C**) in *CDK13* we find that it corresponds to consensus position 10 in the Pkinase  
219 domain (PF00069). At this position in *CDK13* there are two variants reported in ClinVar:  
220 p.Gly714Arg (ClinVar ID: 375738) submitted by (Sifrim et al., 2016), and p.Gly714Asp  
221 (ClinVar ID: 449224) submitted by GeneDX. The first is reported as a *de novo* variant and is  
222 associated to Congenital Heart Defects, Dysmorphic Facial Features, and Intellectual  
223 Developmental Disorder. For the second there is no associated phenotype provided. As  
224 MetaDome annotates variants reported at homologous positions, we can find even more  
225 information for this particular position. At the homologues aligned to this position we find a  
226 variant of identical change in *PRKD1*: p.Gly600Arg (ClinVar ID: 375740) reported as  
227 pathogenic and *de novo* in the same study (Sifrim et al., 2016). It is also associated to Congenital  
228 Heart Defects as well as associated to Ectodermal Dysplasia. There are three more reported  
229 pathogenic variants aligned to this position: *MAK*:p.Gly13Ser (ClinVar ID: 29783) associated to  
230 Retinitis Pigmentosa 62 (Özgül et al., 2011), *PRKCG*:p.Gly360Ser (ClinVar ID: 42129)  
231 associated to Spinocerebellar Ataxia Type14 (Klebe et al., 2005), and *CIT*:p.Gly106Val (ClinVar  
232 ID: 254134) associated to Microcephaly 17, primary, autosomal recessive (Özgül et al., 2011).  
233 These homologously related pathogenic variants and the severity of the associated phenotypes

234 contributes to the evidence that this particular residue may be important at this position. Further  
235 evidence can be found from the fact that in human homologue domains this residue is extremely  
236 conserved. There are 330 unique genomic regions encoding for a codon aligned to this position  
237 (**Supp Data S2**). Only in the gene *PIK3R4* (ENST00000356763.3) does this codon encode for  
238 another residue than Glycine, namely a Threonine at position p.Thr35.

239 In the same way that we explored pathogenic ClinVar variation we can also explore the variation  
240 reported in gnomAD. In *CDK13* at protein position 714 there is no reported variant in gnomAD,  
241 but there are homologously related variations. There are 65 missense variants with average allele  
242 frequency of 1.24E-05 and 76 synonymous with average allele frequency 8.71E-03 and there is  
243 no reported nonsense variation (**Supp Data S1**).

244 When we inspect the tolerance landscape for *CDK13* (**Figure 2A**) we can see that all of the  
245 ClinVar variants (either annotated in *CDK13* or related via homologues) fall within the Pkinase  
246 Pfam protein domain (PF00069). In addition, the protein domain can clearly be seen as more  
247 intolerant to missense variation as compared to other parts of this protein, thereby supporting the  
248 ClinVar variants likely pathogenic role.

## 249 **Conclusion**

250 The MetaDome web server combines resources and information from different fields of expertise  
251 (e.g. genomics and proteomics) in order to increase the power in analysing population and  
252 pathogenic variation by transposing this variation to homologous protein domains. Such a  
253 transfer of information is achieved by a per-position mapping between the GENCODE and  
254 Swiss-Prot databases. 79.4% of the Human Swiss-Prot protein sequences are of identical match  
255 to one or more of 42,116 GENCODE transcripts. This means that 25.7% of the GENCODE

256 transcriptions differ in mRNA but translate to the same Swiss-Prot protein sequence. GENCODE  
257 previously reported that this is due to alternative splicing, of which a substantial proportion only  
258 affect untranslated regions (UTRs) and thus have no impact on the protein-coding part of the  
259 gene (Harrow et al., 2006).

260 MetaDome is especially informative if a variant of interest falls within a protein domain that has  
261 homologues. This is highly likely as 43.6% of the positions in the MetaDome mapping database  
262 are part of a homologous protein domain. Pathogenic missense variation is also highly likely to  
263 fall within a protein domain as we previously observed for 71% of HGMD and 72% of ClinVar  
264 pathogenic missense variants (Wiel et al., 2017). By aggregating variation over protein domain  
265 homologues via MetaDome, the resolution of genetic tolerance at a single base-pair is increased.  
266 Furthermore, we can obtain variation that could disrupt the functionality of a protein domain, as  
267 annotated throughout the entire human genome, which may potentially be disease-causing. It  
268 should be noted, that by aggregating genetic variation in this way the specific context such as  
269 haplotype information or interactions with other proteins may be lost. Aggregation via meta-  
270 domains only encapsulates general biological or molecular functions attributed to the domain.  
271 Nonetheless, we believe MetaDome can be used to better interpret variants of unknown  
272 significance through the use of meta-domains and tolerance landscapes as we have shown in our  
273 example.

274 As more genetic data accumulates in the years to come, MetaDome will become more and more  
275 accurate in predictions of intolerance at the base-pair level and the meta-domain landscapes will  
276 become even more populated with variation found in homologue protein domains. We can  
277 imagine many other ways of integrating this type of information to be helpful for variant  
278 interpretation. Future directions for the MetaDome web server could lead to machine learning

279 empowered variant effect prediction, or visualization of the meta-domain information in a  
280 protein 3D structure.

281 **Methods**

282 **Software architecture of MetaDome**

283 MetaDome is developed in Python v3.5.1 (Rossum & Drake, 2010) and makes use of the Flask  
284 framework v0.12.4 (Ronacher, 2010) for the web service part which communicates between the  
285 front-end, the back-end, and the database. The software architecture (**Supp. Fig S5**) follows the  
286 Domain-driven design paradigm (Evans, 2004). The code is open source and can be found at our  
287 GitHub repository: <https://github.com/cmbi/metadome>. Detailed instructions on how to deploy  
288 the MetaDome web server can be found there too.

289 To ensure MetaDome can be deployed to any environment and provide a high degree of  
290 modularity, we have containerized the application via Docker v17.12.1 (Hykes, 2013). We use  
291 docker-compose v1.17.1 to ensure that different containerized aspects of the MetaDome server  
292 can work together. The following aspects are containerized to this purpose: 1.) The Flask  
293 application, 2.) a PostgreSQL v10 database wherein the mapping database is stored, 3.) a Celery  
294 v4.2.0 task queue management system to facilitate the larger tasks of the MetaDome web-based  
295 user requests, 4.) a Redis v4.0.11 for task result storage, and 5.) RabbitMQ v3.7 to mediate as a  
296 task broker between client and workers. For a full overview of the docker-compose architecture  
297 we refer to **Supp. Fig. S6**.

298 The visualization medium of the MetaDome web server is a fully interactive and responsive  
299 HTML web page. This page is generated by the Flask framework and the navigation aesthetics

300 are made using the CSS framework Bulma v0.7.1 (Thomas, Potekhin, Lauhakari, Shah, &  
301 Berning, 2018). The visualizations of the various landscapes and the schematic protein are  
302 created with JavaScript, JQuery v3.3.1, and the D3 Framework v4.13.0 (Bostock, Ogievetsky, &  
303 Heer, 2011).

304 **Datasets of population and disease-causing genetic variation**

305 MetaDome makes use of single nucleotide variants (SNVs) from population and clinically  
306 relevant genetic variation databases. Population variation was obtained from the gnomAD r2.0.2  
307 VCF file by selecting all synonymous, nonsense, and missense variants that meet the PASS filter  
308 criteria. Variants meeting the PASS criteria are considered to be true variants (Lek et al., 2016).  
309 The variants in the VCF file from ClinVar release 2018 05 03 with disease-causing (Pathogenic)  
310 status are used as the disease-causing SNVs in MetaDome.

311 **Creating the mapping database**

312 MetaDome stores a complete mapping between genomic, protein positions, and all domain  
313 annotations (**Supp. Fig. S7**) in a PostgreSQL relational database (PostgreSQL Global  
314 Development Group, 1996). This mapping is auto-generated and stored in the PostgreSQL  
315 database by the MetaDome web server upon the first run. The genomic positions consist of each  
316 chromosomal position in the protein-coding transcripts of the GENCODE release 19  
317 GRCh37.p13 Basic set (Harrow et al., 2012). The protein positions correspond to protein  
318 sequence positions in the UniProtKB/Swiss-Prot Release 2016\_09 databank entries for the  
319 human species (Boutet et al., 2016). These mappings are created with Protein-Protein BLAST  
320 v2.2.31+ (Camacho et al., 2009) for each protein-coding translation in the GENCODE Basic set  
321 to human canonical and isoform Swiss-Prot protein sequences. We exclude sequences that do not

322 start with a start codon (i.e. ATG encoding for methionine), or end with a stop codon. We  
323 checked if the cDNA sequence of the transcripts match the GENCODE translation via  
324 Biopython's translate function (Cock et al., 2009), if they are not identical than these are  
325 excluded too. The global information on the transcript (e.g. identifiers, sequence length) is  
326 registered in the database in the table 'genes' and, for each Swiss-Prot entry with an identical  
327 sequence match, the global information is stored in the table 'proteins'.

328 Next, for each identical match between translation and Swiss-Prot sequence a ClustalW2 v2.1  
329 (Larkin et al., 2007) alignment is made between these two sequences. Each nucleotide's genomic  
330 position is mapped to the protein position and stored in the 'mappings' table. Each entry in  
331 mapping represents a single nucleotide of a codon and is linked to the corresponding entry in the  
332 'genes' and 'proteins' table (i.e. the corresponding GENCODE translation, transcription and  
333 Swiss-Prot sequence).

334 Each Swiss-Prot sequence in the database is annotated via InterProScan v5.20-59.0 (Finn et al.,  
335 2017) for Pfam-A v30.0 protein domains (Finn et al., 2016) and the results are stored in the  
336 'interpro\_domains' table. After the construction of the database is finished, all meta-domain  
337 alignments can be constructed.

338 **Composing a meta-domain**

339 Meta-domains consist of homologous Pfam protein domain instances that are annotated using  
340 InterproScan. Meta-domains consist of at least two homologous domains. MSAs are made using  
341 a three step process. 1.) Retrieve all sequences for the domain instances, 2.) Retrieve the Pfam  
342 HMM corresponding to the Pfam identifier annotated by InterproScan, and 3.) Use HMMER  
343 3.1b2 (Finn et al., 2015) to align the sequences from the first step. The resulting Stockholm

344 format MSA files can be inspected with alignment visualization software like Jalview  
345 (Waterhouse, Procter, Martin, Clamp, & Barton, 2009). In this Stockholm formatted file, all  
346 columns that correspond to the domain consensus represent the same homologous positions.

347 These Stockholm files are retrieved by the MetaDome web server when a user request meta-  
348 domain information for a position of their interest. Upon retrieval of this Stockholm file, the  
349 mapping database is used to obtain the corresponding genomic positions for each residue. These  
350 genomic positions are subsequently used to retrieve corresponding gnomAD or ClinVar  
351 variation.

### 352 **Computing genetic tolerance and generating a tolerance landscape**

353 The non-synonymous over synonymous ratio, or  $d_N/d_S$  score, is used to quantify genetic  
354 tolerance. This score is based on the observed (obs) missense and synonymous variation in  
355 gnomAD ( $missense_{obs}$  and  $synonymous_{obs}$ ). This score is corrected for the sequence  
356 composition by taking into account the background (bg) of possible missense and synonymous  
357 variants based on the codon table ( $missense_{bg}$  and  $synonymous_{bg}$ ):

$$358 \quad d_N/d_S = \frac{missense_{obs}/missense_{bg}}{synonymous_{obs}/synonymous_{bg}}.$$

359 The tolerance landscape computes this ratio as a sliding window of size 21 (i.e. ten residues  
360 before and ten after the residue of interest) over the entirety of the gene's protein. The edges (e.g.  
361 start and end) are therefore a bit noisy as they are not the result of averaging over a full length  
362 window.

363 **Acknowledgements**

364 This work was in part financially supported by grants from the Netherlands Organization for  
365 Scientific Research (916-14-043 to C.G. and 918-15-667 to J.A.V.), and from the Radboud  
366 Institute for Molecular Life Sciences, Radboud university medical center (R0002793 to G.V.).  
367 We thank Hanka Venselaar for her critically reading of the manuscript.

368 **URLs**

369 MetaDome web service: <https://stuart.radboudumc.nl/metadome>

370 GENCODE: <https://www.gencodegenes.org/>

371 InterPro: <https://www.ebi.ac.uk/interpro/>

372 Pfam: <https://pfam.xfam.org/>

373 gnomAD: <http://gnomad.broadinstitute.org/>

374 ClinVar: <https://www.ncbi.nlm.nih.gov/clinvar/>

375 GitHub repository: <https://github.com/cmbi/metadome>

## 376 **References**

377 Altschul, S. F., Gish, W., Miller, W., Myers, E. W., & Lipman, D. J. (1990). Basic local  
378 alignment search tool. *Journal of Molecular Biology*, 215(3), 403–410.  
379 [https://doi.org/10.1016/S0022-2836\(05\)80360-2](https://doi.org/10.1016/S0022-2836(05)80360-2)

380 Amr, S. S., Al Turki, S. H., Lebo, M., Sarmady, M., Rehm, H. L., & Abou Tayoun, A. N. (2016).  
381 Using large sequencing data sets to refine intragenic disease regions and prioritize clinical  
382 variant interpretation. *Genetics in Medicine: Official Journal of the American College of*  
383 *Medical Genetics*, (July), 1–9. <https://doi.org/10.1038/gim.2016.134>

384 Ashenberg, O., Gong, L. I., & Bloom, J. D. (2013). Mutational effects on stability are largely  
385 conserved during protein evolution. *Proceedings of the National Academy of Sciences of the*  
386 *United States of America*, 110(52), 21071–6. <https://doi.org/10.1073/pnas.1314781111>

387 Bostock, M., Ogievetsky, V., & Heer, J. (2011). D<sup>3</sup>: Data-Driven Documents. *IEEE Transactions*  
388 *on Visualization and Computer Graphics*, 17(12), 2301–9.  
389 <https://doi.org/10.1109/TVCG.2011.185>

390 Boutet, E., Lieberherr, D., Tognolli, M., Schneider, M., Bansal, P., Bridge, A. J., ... Xenarios, I.  
391 (2016). UniProtKB/Swiss-Prot, the Manually Annotated Section of the UniProt  
392 KnowledgeBase: How to Use the Entry View. *Methods in Molecular Biology (Clifton,*  
393 *N.J.)*, 1374, 23–54. [https://doi.org/10.1007/978-1-4939-3167-5\\_2](https://doi.org/10.1007/978-1-4939-3167-5_2)

394 Camacho, C., Coulouris, G., Avagyan, V., Ma, N., Papadopoulos, J., Bealer, K., & Madden, T.  
395 L. (2009). BLAST+: architecture and applications. *BMC Bioinformatics*, 10(1), 421.  
396 <https://doi.org/10.1186/1471-2105-10-421>

397 Cock, P. J. A., Antao, T., Chang, J. T., Chapman, B. A., Cox, C. J., Dalke, A., ... de Hoon, M. J.  
398 L. (2009). Biopython: freely available Python tools for computational molecular biology  
399 and bioinformatics. *Bioinformatics (Oxford, England)*, 25(11), 1422–3.  
400 <https://doi.org/10.1093/bioinformatics/btp163>

401 Evans, E. (2004). *Domain-driven design: tackling complexity in the heart of software*. Addison-  
402 Wesley Professional.

403 Finn, R. D., Attwood, T. K., Babbitt, P. C., Bateman, A., Bork, P., Bridge, A. J., ... Mitchell, A.  
404 L. (2017). InterPro in 2017—beyond protein family and domain annotations. *Nucleic Acids  
405 Research*, 45(D1), D190–D199. <https://doi.org/10.1093/nar/gkw1107>

406 Finn, R. D., Clements, J., Arndt, W., Miller, B. L., Wheeler, T. J., Schreiber, F., ... Eddy, S. R.  
407 (2015). HMMER web server: 2015 update. *Nucleic Acids Research*, 43(W1), W30–W38.  
408 <https://doi.org/10.1093/nar/gkv397>

409 Finn, R. D., Coggill, P., Eberhardt, R. Y., Eddy, S. R., Mistry, J., Mitchell, A. L., ... Bateman, A.  
410 (2016). The Pfam protein families database: towards a more sustainable future. *Nucleic  
411 Acids Research*, 44(D1), D279–D285. <https://doi.org/10.1093/nar/gkv1344>

412 Fu, W., O'Connor, T. D., Jun, G., Kang, H. M., Abecasis, G., Leal, S. M., ... Akey, J. M. (2012).  
413 Analysis of 6,515 exomes reveals the recent origin of most human protein-coding variants.  
414 *Nature*, 493(7431), 216–220. <https://doi.org/10.1038/nature11690>

415 Ge, X., Gong, H., Dumas, K., Litwin, J., Phillips, J. J., Waisfisz, Q., ... Shieh, J. T. C. (2016).  
416 Missense-depleted regions in population exomes implicate ras superfamily nucleotide-  
417 binding protein alteration in patients with brain malformation. *Npj Genomic Medicine*, 1(1),

418 16036. <https://doi.org/10.1038/npjgenmed.2016.36>

419 Ge, X., Kwok, P.-Y., & Shieh, J. T. C. (2015). Prioritizing genes for X-linked diseases using  
420 population exome data. *Human Molecular Genetics*, 24(3), 599–608.  
421 <https://doi.org/10.1093/hmg/ddu473>

422 Gilissen, C., Hehir-Kwa, J. Y., Thung, D. T., van de Vorst, M., van Bon, B. W. M., Willemsen,  
423 M. H., ... Veltman, J. A. (2014). Genome sequencing identifies major causes of severe  
424 intellectual disability. *Nature*, 511(7509), 344–347. <https://doi.org/10.1038/nature13394>

425 Gussow, A. B., Petrovski, S., Wang, Q., Allen, A. S., & Goldstein, D. B. (2016). The intolerance  
426 to functional genetic variation of protein domains predicts the localization of pathogenic  
427 mutations within genes. *Genome Biology*, 17(1), 9. <https://doi.org/10.1186/s13059-016-0869-4>

429 Harrow, J., Denoeud, F., Frankish, A., Reymond, A., Chen, C.-K., Chrast, J., ... Guigo, R.  
430 (2006). GENCODE: producing a reference annotation for ENCODE. *Genome Biology*, 7  
431 *Suppl 1*(Suppl 1), S4.1-9. <https://doi.org/10.1186/gb-2006-7-s1-s4>

432 Harrow, J., Frankish, A., Gonzalez, J. M., Tapanari, E., Diekhans, M., Kokocinski, F., ...  
433 Hubbard, T. J. (2012). GENCODE: The reference human genome annotation for The  
434 ENCODE Project. *Genome Research*, 22(9), 1760–1774.  
435 <https://doi.org/10.1101/gr.135350.111>

436 Hykes, S. (2013). Docker. San Francisco: Docker, Inc. Retrieved from <https://www.docker.com/>

437 Karczewski, K. J., Weisburd, B., Thomas, B., Solomonson, M., Ruderfer, D. M., Kavanagh, D.,  
438 ... MacArthur, D. G. (2017). The ExAC browser: Displaying reference data information

439 from over 60 000 exomes. *Nucleic Acids Research*, 45(D1), D840–D845.

440 <https://doi.org/10.1093/nar/gkw971>

441 Klebe, S., Durr, A., Rentschler, A., Hahn-Barma, V., Abele, M., Bouslam, N., ... Stevanin, G.

442 (2005). New mutations in protein kinase C $\gamma$  associated with spinocerebellar ataxia type 14.

443 *Annals of Neurology*, 58(5), 720–729. <https://doi.org/10.1002/ana.20628>

444 Landrum, M. J., Lee, J. M., Benson, M., Brown, G., Chao, C., Chitipiralla, S., ... Maglott, D. R.

445 (2016). ClinVar: public archive of interpretations of clinically relevant variants. *Nucleic*

446 *Acids Research*, 44(D1), D862-8. <https://doi.org/10.1093/nar/gkv1222>

447 Larkin, M. A., Blackshields, G., Brown, N. P., Chenna, R., McGettigan, P. A., McWilliam, H.,

448 ... Higgins, D. G. (2007). Clustal W and Clustal X version 2.0. *Bioinformatics*, 23(21),

449 2947–2948. <https://doi.org/10.1093/bioinformatics/btm404>

450 Lek, M., Karczewski, K. J., Minikel, E. V., Samocha, K. E., Banks, E., Fennell, T., ...

451 MacArthur, D. G. (2016). Analysis of protein-coding genetic variation in 60,706 humans.

452 *Nature*, 536(7616), 285–291. <https://doi.org/10.1038/nature19057>

453 Lelieveld, S. H., Wiel, L., Venselaar, H., Pfundt, R., Vriend, G., Veltman, J. A., ... al., et.

454 (2017). Spatial Clustering of de Novo Missense Mutations Identifies Candidate

455 Neurodevelopmental Disorder-Associated Genes. *The American Journal of Human*

456 *Genetics*, 8(0), 52–56. <https://doi.org/10.1016/j.ajhg.2017.08.004>

457 Li, W. H., Wu, C. I., & Luo, C. C. (1985). A new method for estimating synonymous and

458 nonsynonymous rates of nucleotide substitution considering the relative likelihood of

459 nucleotide and codon changes. *Molecular Biology and Evolution*, 2(2), 150–74.

460 <https://doi.org/10.1128/AAC.03728-14>

461 NHLBI GO Exome Sequencing Project (ESP). (2011). Exome Variant Server. Retrieved May  
462 14, 2015, from <http://evs.gs.washington.edu/EVS/>

463 Özgül, R. K., Siemiatkowska, A. M., Yücel, D., Myers, C. A., Collin, R. W. J., Zonneveld, M.  
464 N., ... Corbo, J. C. (2011). Exome sequencing and cis-regulatory mapping identify  
465 mutations in MAK, a gene encoding a regulator of ciliary length, as a cause of retinitis  
466 pigmentosa. *American Journal of Human Genetics*, 89(2), 253–264.  
467 <https://doi.org/10.1016/j.ajhg.2011.07.005>

468 Petrovski, S., Wang, Q., Heinzen, E. L., Allen, A. S., & Goldstein, D. B. (2013). Genic  
469 Intolerance to Functional Variation and the Interpretation of Personal Genomes. *PLoS  
470 Genetics*, 9(8), e1003709. <https://doi.org/10.1371/journal.pgen.1003709>

471 PostgreSQL Global Development Group. (1996). PostgreSQL. PostgreSQL Global Development  
472 Group. Retrieved from <https://www.postgresql.org/>

473 Ronacher, A. (2010). Flask. Retrieved from <http://flask.pocoo.org/>

474 Rossum, G. Van, & Drake, F. L. (2010). Python Tutorial. *History*, 42(4), 1–122.  
475 [https://doi.org/10.1111/j.1094-348X.2008.00203\\_7.x](https://doi.org/10.1111/j.1094-348X.2008.00203_7.x)

476 Sifrim, A., Hitz, M.-P., Wilsdon, A., Breckpot, J., Turki, S. H. Al, Thienpont, B., ... Hurles, M.  
477 E. (2016). Distinct genetic architectures for syndromic and nonsyndromic congenital heart  
478 defects identified by exome sequencing. *Nature Genetics*, 48(9), 1060–5.  
479 <https://doi.org/10.1038/ng.3627>

480 Stenson, P. D., Mort, M., Ball, E. V., Evans, K., Hayden, M., Heywood, S., ... Cooper, D. N.

481 (2017). The Human Gene Mutation Database: towards a comprehensive repository of  
482 inherited mutation data for medical research, genetic diagnosis and next-generation  
483 sequencing studies. *Human Genetics*, 136(6), 1–13. <https://doi.org/10.1007/s00439-017-1779-6>

485 Thomas, J., Potekhin, O., Lauhakari, M., Shah, A., & Berning, D. (2018). *Creating Interfaces*  
486 with *Bulma*. (T. Mott & D. Berning, Eds.). Santa Rosa: Bleeding Edge Press. Retrieved  
487 from <https://bleedingedgepress.com/>

488 Waterhouse, A. M., Procter, J. B., Martin, D. M. A., Clamp, M., & Barton, G. J. (2009). Jalview  
489 Version 2--a multiple sequence alignment editor and analysis workbench. *Bioinformatics*,  
490 25(9), 1189–1191. <https://doi.org/10.1093/bioinformatics/btp033>

491 Wiel, L., Venselaar, H., Veltman, J. A., Vriend, G., & Gilissen, C. (2017). Aggregation of  
492 population-based genetic variation over protein domain homologues and its potential use in  
493 genetic diagnostics. *Human Mutation*, (May), 1–10. <https://doi.org/10.1002/humu.23313>

494 Yang, & Bielawski. (2000). Statistical methods for detecting molecular adaptation. *Trends in*  
495 *Ecology & Evolution*, 15(12), 496–503. [https://doi.org/10.1016/S0169-5347\(00\)01994-7](https://doi.org/10.1016/S0169-5347(00)01994-7)

496 Yang, Z., Swanson, W. J., & Vacquier, V. D. (2000). Maximum-likelihood analysis of molecular  
497 adaptation in abalone sperm lysin reveals variable selective pressures among lineages and  
498 sites. *Molecular Biology and Evolution*, 17(10), 1446–55.  
499 <https://doi.org/10.1093/oxfordjournals.molbev.a026245>

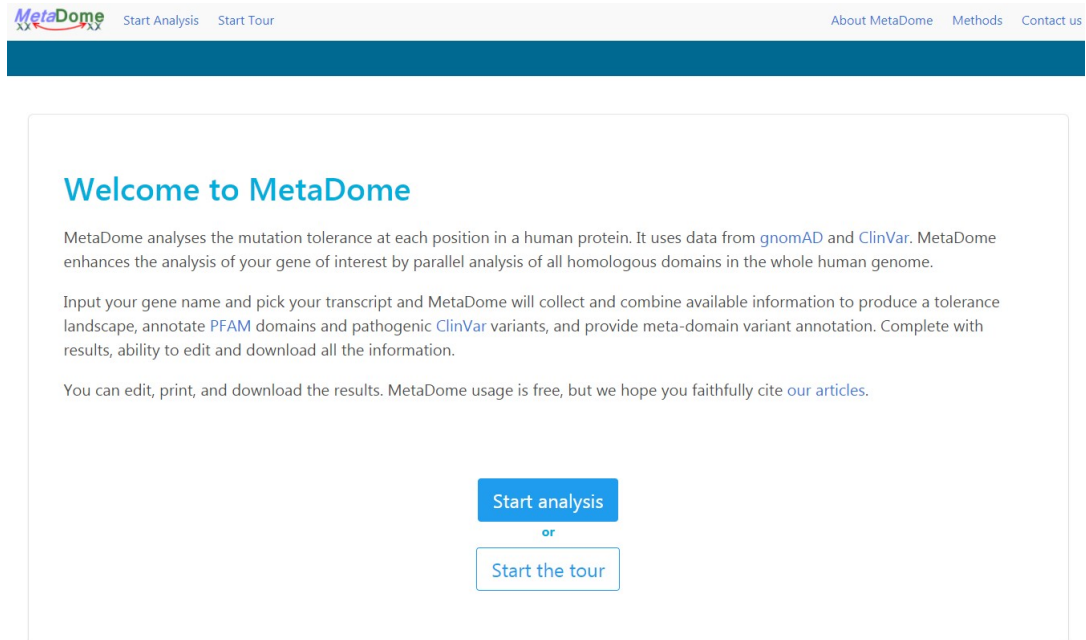
500

501

502 **Supplemental Figures**

503

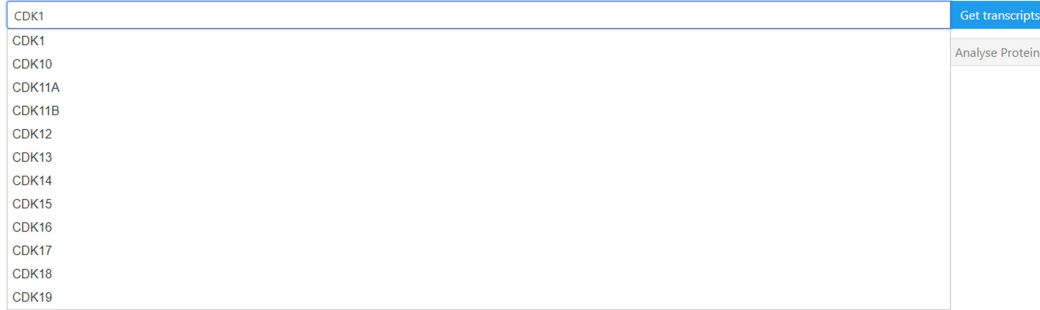
504 **Supp Fig. S1. Welcome page**



505

506 The welcome page of MetaDome is the entry point to the rest of the web server. Here the  
507 navigation bar is located at the top that eases navigation throughout the rest of the web pages.  
508 From here the user can start the interactive tour or an analysis.

509 **Supp Fig. S2. Gene symbol auto-completion**

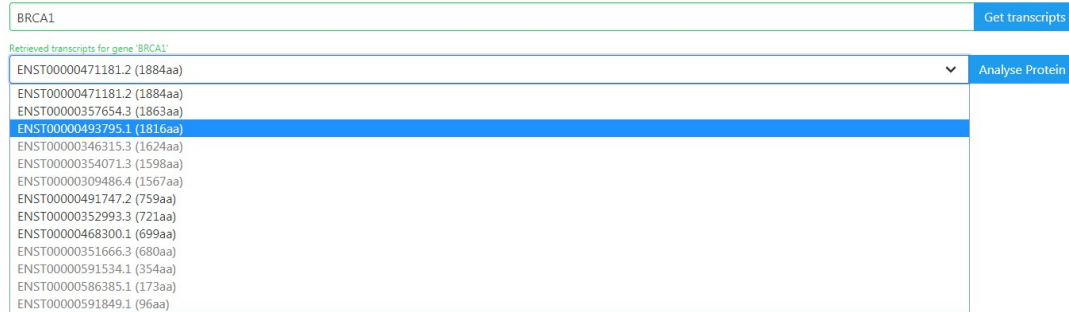


510

511 The auto-completion of gene symbols is based on all gene symbols present in the mapping  
512 database. The auto-completion will start once the user has entered three characters in the input  
513 field and is interactive (e.g. you can click on the gene that is of your interest).

514

515 **Supp Fig. S3. Dropdown box containing transcript identifiers**



BRCA1

Retrieved transcripts for gene 'BRCA1'

ENST00000471181.2 (1884aa)  
ENST00000471181.2 (1884aa)  
ENST00000357654.3 (1863aa)  
**ENST00000493795.1 (1816aa)**  
ENST00000346315.3 (1624aa)  
ENST00000354071.3 (1598aa)  
ENST00000309486.4 (1567aa)  
ENST00000491747.2 (759aa)  
ENST00000352993.3 (721aa)  
ENST00000468300.1 (699aa)  
ENST00000351666.3 (680aa)  
ENST00000591534.1 (354aa)  
ENST00000586385.1 (173aa)  
ENST00000591849.1 (96aa)

Get transcripts

Analyse Protein

516

517 The result of clicking the 'Get transcripts' button for the *BRCA1* gene. Here a success message is  
518 displayed in green, which means that the gene is present in the database. The resulting transcripts  
519 are ordered by amino acid (aa) length and the longest transcripts are at the top. The greyed-out  
520 transcripts are not suitable for further analysis in the web server.

521 **Supp Fig. S4. Dropdown box containing transcript identifiers**

**Positional information (p.883)**  
Gene: CDK13 (transcript: [ENST00000181839.4](#), protein: [Q14004](#))

**Location details**  
Chr: chr7, strand: +  
Gene: g.40102471-40102473  
Protein: p.883 Glu  
cDNA: c.2647-2649 GAA  
Position is part of protein domain(s): [PF00069](#)

**Known pathogenic ClinVar SNVs at position**  
No ClinVar SNVs found at position

**Meta-domain information for domain PF00069:**  
Aligned to consensus position 167, related to 347 other codons throughout the genome (with a 98.6% alignment coverage).

**Pathogenic ClinVar SNVs at homologous positions:**

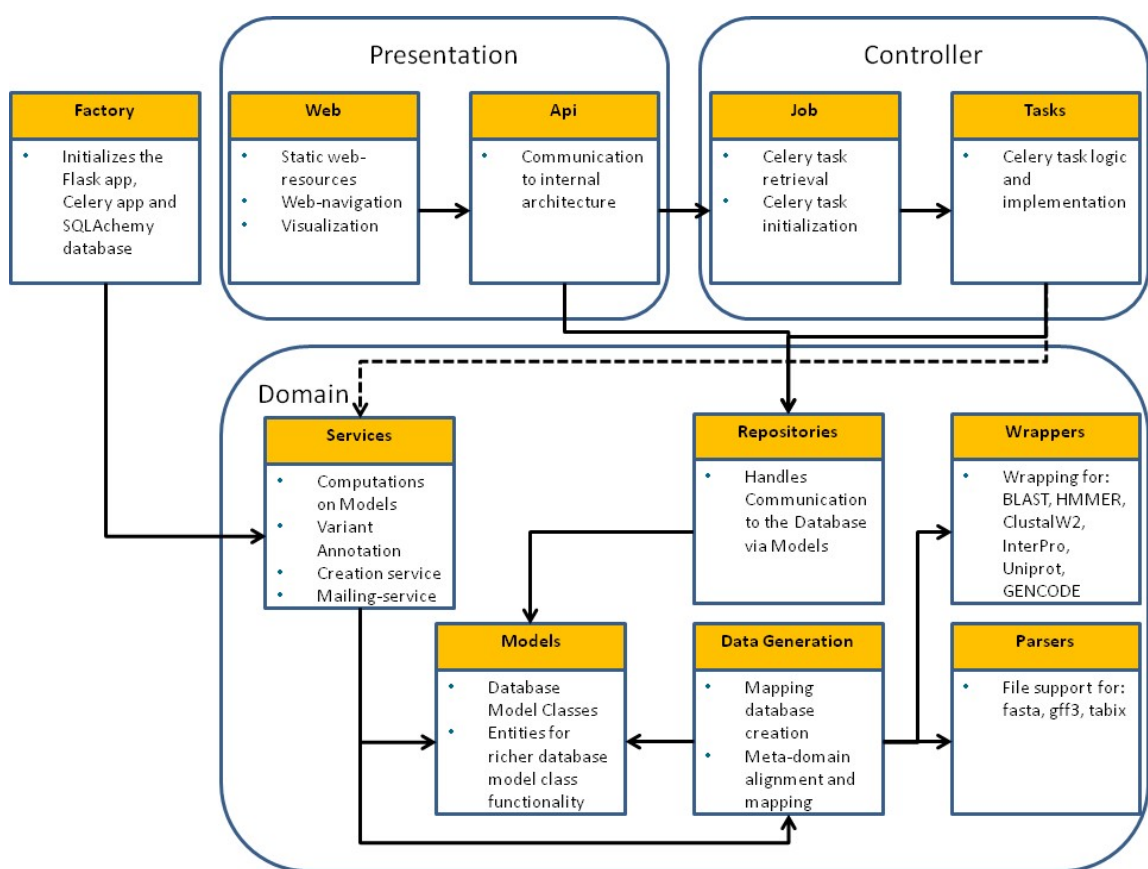
Chr	Pos	Codon change	Residue change	Type	ClinVar ID
chrX	g.20206006-20206008	GAA>TAA	Glu>*	nonsense	<a href="#">522031</a>
chr2	g.203397335-203397337	GAA>CAA	Glu>Gln	missense	<a href="#">425884</a>
chr2	g.203397335-203397337	GAA>AAA	Glu>Lys	missense	<a href="#">425883</a>
chr2	g.203397335-203397337	GAA>GCA	Glu>Ala	missense	<a href="#">425885</a>
chrX	g.18602460-18602462	GAA>GCA	Glu>Ala	missense	<a href="#">156604</a>
chr5	g.149631594-149631596	GAA>GTA	Glu>Val	missense	<a href="#">430914</a>
chr2	g.203397335-203397337	GAA>GTA	Glu>Val	missense	<a href="#">425887</a>
chr2	g.203397335-203397337	GAA>GGA	Glu>Gly	missense	<a href="#">425886</a>

**Variants in gnomAD SNVs at homologous positions:**

Chr	Pos	Codon change	Residue change	Type	Allele Frequency
chr11	g.77047242-77047244	GAG>AAG	Glu>Lys	missense	0.000004
chr20	g.30418874-30418876	GAG>GAA	Glu>Glu	synonymous	0.000065
chr10	g.49628330-49628332	GAG>GAA	Glu>Glu	synonymous	0.000004
chr3	g.170009705-170009707	GAA>GAG	Glu>Glu	synonymous	0.000008

522  
523 The positional information overview provides detailed positional information for position  
524 p.Glu883. We can observe that it is aligned to consensus position 167 in the Pkinase Pfam  
525 protein domain. This consensus position has 98.6% alignment coverage. On this position no  
526 ClinVar pathogenic variants are found in *CDK13*, but on homologous positions there are eight  
527 pathogenic ClinVar variants annotated.  
528

529 **Supp Fig. S5. The software architecture of the MetaDome web server**

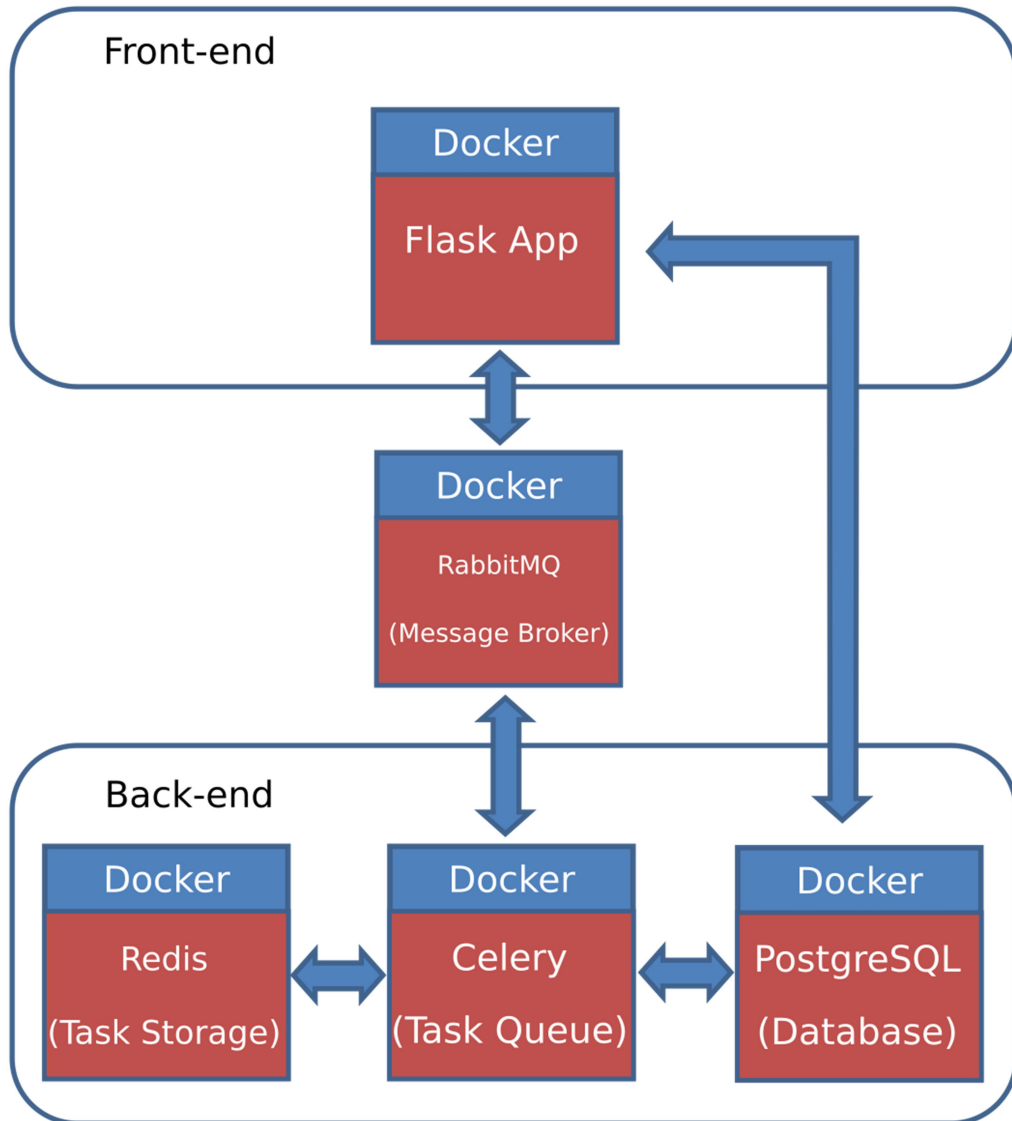


530

531 A high-level overview of the software architecture of the MetaDome web server. The  
532 architecture follows closely the Domain-driven design paradigm. In this architecture we make  
533 use of three distinct layers with separated responsibilities. The Presentation layer is responsible  
534 for the user interface and external communication handling. This layer takes care of all the  
535 visualizations in the web interface and any user input that needs further validation or that  
536 requires starting a celery job. In the controller layer all communication is handled from the  
537 MetaDome server to the Celery task queue. Job here instantiates and checks the status of jobs in  
538 the Celery queue that are initialized from Tasks. The Domain layer contains all the domain-  
539 knowledge of the MetaDome application. Here Repositories is the outside connection for  
540 approaching the internal database, so no domain knowledge is needed by the Presentation layer.

541 The services take care of various computations on the data from Models and contains  
542 functionality to create the database via Data Generation. The Factory is outside the layers, but  
543 initializes the configuration to run the MetaDome server (e.g. connections to the PostgreSQL and  
544 Celery Docker containers and start of the Flask web service).

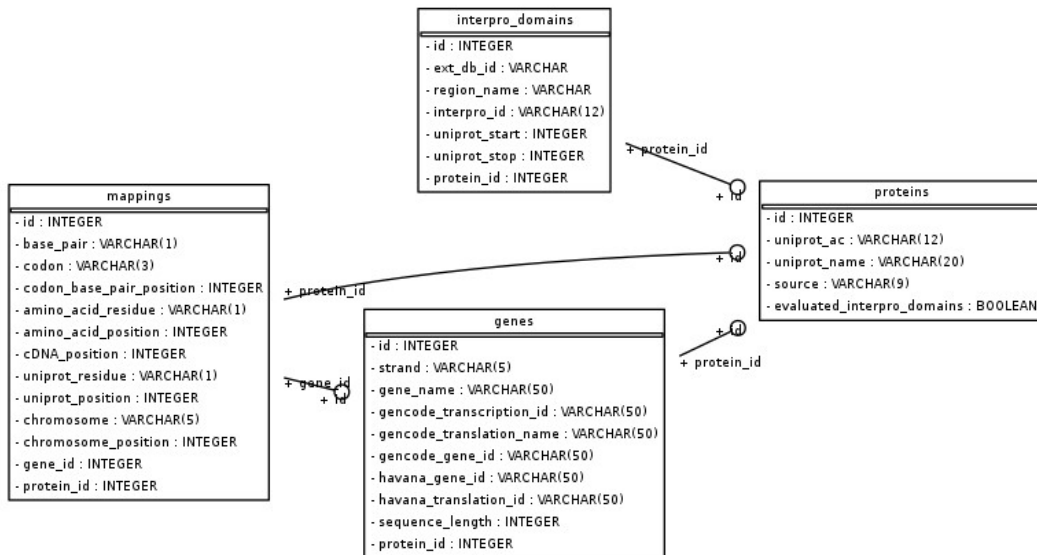
545 Supp Fig. S6. The internal docker network architecture of the MetaDome web server



546

547 Metadome makes use of several docker containers that work jointly via docker-compose to  
548 provide various degrees of functionality. The Flask App docker container is responsible for  
549 hosting the MetaDome visual interface and at the first run it will create the mapping database.  
550 The Flask docker container communicates via the RabbitMQ service, which serves as a message  
551 broker, to the Celery docker container. This Celery container keeps track of the large tasks and  
552 the results of those tasks are temporarily stored in the Redis server. The PostgreSQL container  
553 houses the database containing the mapping between GENCODE transcripts and Swiss-Prot.

554 **Supp Fig. S7. The internal database architecture for the MetaDome web server**



555

556 The backbone of the MetaDome web server is a relational PostgreSQL database. This schematic  
557 representation of the tables present an overview of the relations in the data and what type of  
558 information is stored for each data entry. The table ‘mappings’ contain entries of a per-  
559 chromosome position (per gene) entries with codon to amino acid residue information. This is  
560 done for each of the nucleotides in a codon. The ‘genes’ table represent information from each of  
561 the transcripts present in the GENCODE database and the ‘proteins’ table correspond to global  
562 information on entries from the UniProtKB/Swiss-Prot databank. The ‘interpro\_domains’ table  
563 can support any type of interpro domain, but for the purpose of MetaDome contain solely the  
564 Pfam protein domains. This database brings together genomic and protein positions that can be  
565 further used for annotation purposes.

566